Electrostatic wave modulation in collisional pair-ion plasmas

Arnab Sikdar, Ashish Adak, Samiran Ghosh, and Manoranjan Khan

Citation: Physics of Plasmas **25**, 052303 (2018); doi: 10.1063/1.4997224
View online: https://doi.org/10.1063/1.4997224
View Table of Contents: http://aip.scitation.org/toc/php/25/5
Published by the American Institute of Physics

PHYSICS OF PLASMAS 25, 052303 (2018)

Electrostatic wave modulation in collisional pair-ion plasmas

Arnab Sikdar,[1,a)] Ashish Adak,[2,b)] Samiran Ghosh,[3,c)] and Manoranjan Khan[2,d)]
[1]Department of Mathematics, Calcutta Institute of Engineering and Management, 24/1A Chandi Ghosh Road, Kolkata 700040, India
[2]Department of Instrumentation Science, Jadavpur University, Kolkata 700032, India
[3]Department of Applied Mathematics, University of Calcutta, 92, Acharya Prafulla Chandra Road, Kolkata 700009, India

(Received 22 July 2017; accepted 29 April 2018; published online 15 May 2018)

The effects of ion-neutral collision on the electrostatic wave packets in the absence of the magnetic field in a pair-ion plasma have been investigated. Considering a two-fluid plasma model with the help of the standard perturbation technique, two distinct electrostatic modes have been observed, namely, a low-frequency ion acoustic mode and a high-frequency ion plasma mode. The dynamics of the modulated wave is governed by a damped nonlinear Schrödinger equation. Damping of the soliton occurs due to the ion-neutral collision. The analytical and numerical investigation reveals that the ion acoustic mode is both stable and unstable, which propagates in the form of dark solitons and bright solitons, respectively, whereas the ion plasma mode is unstable, propagating in the form of a bright soliton. Results are discussed in the context of the fullerene pair-ion plasma experiments. *Published by AIP Publishing.* https://doi.org/10.1063/1.4997224

I. INTRODUCTION

Pair plasmas consisting of positive and negative ions (without electrons) with equal masses have been studied intensively in the last few decades in theory[1–7] and in experiments.[8–11] The physics of pair plasmas is completely different from that of the normal electron ion plasmas. Pair plasmas are benefited by the space time symmetry in contrast to the normal electron ion plasmas with a wide mass difference. The symmetry arises due to the same mobility of the charged particles in electromagnetic fields. As a result, varieties of new physical phenomena have been studied in such symmetric pair plasmas. Pair plasmas consisting of electrons and positrons exist in the pulsar magnetosphere, early universe, active galaxy,[12–15] and inertial confinement fusion reactor using ultraintense lasers.[16] Although pair plasmas consisting of electrons and positrons can be produced experimentally, it is very difficult to identify the collective modes because of the annihilation time, which is short in comparison to the plasma period.[17]

However, in pair-ion plasmas composed of positive and negative ions, larger time scale can be considered. Therefore, no need to worry about the annihilation time in pair-ion plasmas. Such pair ion plasmas have been produced experimentally[18] by using positive and negative fullerene ions ($C_{60}^{\pm}$) as the ion source. These fullerene ions maintain a typical geometric arrangement containing 60 carbon atoms. This experimental result allows us to analyze new collective modes in pair-ion plasmas in a controlled situation. There is a huge prospect of usefulness of such types of pair-ion plasmas in nanotechnology and for the synthesis of dimers directly from carbon allotropes.[19]

In experiments, three types of electrostatic collective modes were observed in such pair ion plasmas:[20–23] (a) low-frequency ion acoustic wave (IAW), (b) high-frequency ion plasma wave (IPW), and (c) intermediate-frequency wave (IFW). The frequency of IFW lies between the frequency of IAW and IPW. Theoretical studies of linear electrostatic and electromagnetic modes in pair plasmas have been carried out taking the kinetic[24] or the fluid dynamical model.[25–27] In fullerene pair-ion plasmas, when negative C_{60}^{-} ions collide with positive C_{60}^{+} ions and/or neutral fullerene, dimers C_{60}, C_{120}, and C_{121} may be produced as a collisional product.[28,29] These dimers have acquired an interest from the standpoint of applications to nanoscale magnetic materials,[30] nanotechnology, and fusion plasmas.[29]

Recently, the effects of collisions with neutrals on propagation dynamics of linear electrostatic modes in pair-ion plasmas have been extensively investigated in the presence of a uniform external magnetic field.[27] In such a system, nonlinearity acts into play when wave amplitude becomes large. An intrinsic character of the nonlinear wave is the self-interactions. These self-interactions introduce self-focusing effects (modulational instability). In the absence of collisions, the wave modulation characteristics of electrostatic modes have already been investigated in pair-ion plasmas.[4,31] These investigations motivate us to investigate the nonlinear electrostatic wave modulations in one-spatial dimension in a pair-ion plasma in the presence of ion-neutral collision.

To study the nonlinear propagation of electrostatic modes, we have taken the two fluid equations to describe the model for two ion species and employed the standard reductive perturbation technique (RPT). Two distinct modes are derived the same as the experimental observation, namely, ion acoustic wave $\omega_1^2 = C_s^2 k^2$ (here, ω_1, k, and C_s denote the frequency, wave number, and ion acoustic speed, respectively) and a ion plasma wave $\omega_2^2 = 2\omega_p^2 + C_s^2 k^2$ with a cutoff frequency $\omega_2(k=0) = \sqrt{2}\omega_p$ (here, ω_p is the characteristic plasma

a)arnabs.ju@gmail.com
b)ashish_adak@yahoo.com
c)sran_g@yahoo.com
d)mkhan.ju@gmail.com

frequency, common for both positive and negative ions). Finally, with the help of RPT, we have derived a dissipative (here damped) nonlinear Schrödinger equation (NLSE). Damping arises due to the ion-neutral collision. After solving this damped NLSE numerically and analytically, we have obtained bright solitons and dark solitons. Also, we have observed that the damping causes the soliton (bright and dark) amplitude to decay with time.

The outline of this paper is as follows: in Sec. II, we demonstrate the complete set of two fluid equations to describe the model. In Sec. III, we derive the damped NLSE using RPT. In Sec. IV, we discuss the effect of ion-neutral collision on modulational instability. In Sec. V, we elaborately discuss about the soliton solutions and the collisional effects on these solutions. Finally, the results are summarized in Sec. VI.

II. PHYSICAL ASSUMPTIONS AND BASIC EQUATIONS

We have considered a homogeneous unbounded and unmagnetized pair-ion plasma system. The plasma constituents are positive and negative fullerene ions (C_{60}^{+} and C_{60}^{-}) without electrons. As per the experimental observations,[20–23] we have considered pair-ion plasmas with equal mass $m_+ = m_- = m(\text{say})$ [where $m_\pm$ is the positive (negative) ion mass] but slightly different [range of $(0.3-0.5)$eV] in temperature $T_+ \neq T_-$ [where $T_\pm$ is the positive (negative) ion temperature]. We have assumed that the plasma is in the equilibrium state at $-\infty$, where electrostatic potential $\phi = 0$, positive ion number density $n_+ = n_{+0}$, and negative ion number density $n_- = n_{-0}$. The plasma is overall quasi-neutral, and we have assumed that the ions are singly charged, and so, in equilibrium, the quasineutrality condition is satisfied, i.e., $n_{+0} = n_{-0} = n_0$ (say).

Before going to the details of the physical model, we have introduced a new temperature variable $T=(T_+ + T_-)/2$. We have taken an explicit density dependence of the pressure in the form $p_\pm = Cn_\pm^{\gamma}$, where γ is the ratio of the two specific heats and C is a constant. As $\gamma = (f+2)/f$, where f is the number of degrees of freedom, in one dimensional cases, we have considered $\gamma = 3$ for one degree of freedom. In a weakly ionized pair-ion plasma, ions (positive and negative) suffer collisions with neutrals and with themselves. In a pair-ion (with equal mass and different temperatures) plasma, the positive (negative) ion-neutral collision frequency ($\nu_{\pm n}$) can be estimated[32] as

$$\nu_{\pm n} = n_n \sigma_{\pm n} \sqrt{\frac{k_B T_\pm}{m}}\ \mathrm{s}^{-1}, \tag{1}$$

where n_n is the neutral density and $\sigma_{\pm n} \sim 5\times 10^{-15}\,\mathrm{cm}^2$ is the scattering cross section. The positive ion-negative ion collision frequency ($\nu_\pm^c$) can be estimated[32] as

$$\nu_\pm^c = 1.8\times 10^{-19}\left[\frac{n_0 e^4 \ln\Lambda}{\sqrt{m}\,T_\pm^{3/2}}\right]\mathrm{s}^{-1}, \tag{2}$$

where $\ln\Lambda \sim (10-20)$ is the Coulomb Logarithm. Experimental observations[18,20–23] reveal that in equal mass pair-ion plasmas, the temperature of positive and negative ions is slightly different [range of $(0.3-0.5)$eV] due to the different charging processes. Numerical estimations show that within the observed temperature range, $\nu_{\pm n} \gg \nu_\pm^c$, and therefore, we consider only the ion-neutral collisions.

We have taken all dependent variables as functions of coordinate variable x and time variable t. Therefore, the normalized two-fluid equations for the pair-ion plasmas with ion-neutral collision are as follows:

$$\frac{\partial n_\pm}{\partial t} + \frac{\partial}{\partial x}(n_\pm u_\pm) = 0, \tag{3}$$

$$\frac{\partial u_\pm}{\partial t} + u_\pm \frac{\partial u_\pm}{\partial x} = \mp \frac{\partial \phi}{\partial x} - \sigma_\pm n_\pm \frac{\partial n_\pm}{\partial x} - \tilde{\nu}_{\pm n} u_\pm, \tag{4}$$

$$\frac{\partial^2 \phi}{\partial x^2} = n_- - n_+, \tag{5}$$

where the physical parameters $\sigma_\pm = T_\pm/T$ and $\tilde{\nu}_{\pm n} = \nu_{\pm n}/\omega_p$. The space and time coordinates are normalized by the plasma Debye length (λ_D) and the inverse of plasma frequency (ω_p), respectively. The variable number density (n), electrostatic potential (ϕ), and velocity ($u_\pm$) of ions are normalized by n_0, T/e, and acoustic speed (C_s), respectively. The plasma parameters are the Debye length $\lambda_D = (\epsilon_0 \gamma T/n_0 e^2)^{1/2}$ and plasma frequency $\omega_p = (n_0 e^2/\epsilon_0 m)^{1/2}$, where ϵ_0 is the permittivity in free space. This defines the acoustic speed $C_s (= \omega_p \lambda_D) = (\gamma T/m)^{1/2}$.

III. NONLINEAR EVOLUTION EQUATIONS

In order to analyze the propagation characteristics of nonlinear modulated waves in a pair-ion plasma from the basic model, Eqs. (1)–(3), we introduce the following slow space and time scales to observe the slow variation of modulated wave amplitude:[33]

$$\xi = \epsilon(x - \lambda t), \quad \tau = \epsilon^2 t, \tag{6}$$

where λ is the group velocity of the propagated wave to be determined later by the compatibility condition and ϵ is a small real parameter that characterizes the strength of nonlinearity. We expand all the physical quantities $n_\pm$, $u_\pm$, and ϕ in powers of ϵ in the following way:

$$A_l = A_0 + \sum_{n=1}^{\infty} \epsilon^n \sum_{l=-\infty}^{\infty} A_l^{(n)}(\xi,\tau)\exp\left(il(kx-\omega t)\right). \tag{7}$$

The reality condition for all physical quantities is $A_{-l}^{(n)} = (A_l^{(n)})^*$; the superscript star denotes the complex conjugates and $A_l^{(n)}$ stands for $n_{\pm,l}^{(n)}$, $u_{\pm,l}^{(n)}$, and ϕ.

Note that in equal mass pair-ion plasmas, the collective modes of IAWs in the presence of collisions are not yet observed in any experiment. Therefore, to incorporate the ion-neutral collisional effects in the nonlinear regime, we consider ($\nu_{\pm n}/\omega_p \ll 1$), i.e., since we assumed that the ion-neutral collision frequency is much smaller than the plasma frequency. Thus, for consistency (between the assumption and perturbation), we consider the following scaling:

$$\tilde{\nu}_{\pm n} \equiv \frac{\nu_{\pm n}}{\omega_p} = \nu_{\pm}\epsilon^2, \tag{8}$$

where $\nu_{\pm}$ is the proportionality constant which defines the normalized ion-neutral collision frequencies for positive and negative ions.

Now, to obtain the nth-order reduced equations (B1)–(B3) (details are given in Appendix B), we substitute the stretched variables [Eq. (4)], the expansion of the physical quantities [Eq. (5)], and the scaling [Eq. (6)] into the normalized Eqs. (1)–(3). For the first order (n = 1), first harmonics (l = 1), we obtain the following set of equations:

$$u^{(1)}_{\pm,1} = \frac{\omega}{k} n^{(1)}_{\pm,1}, \tag{9}$$

$$-\omega u^{(1)}_{\pm,1} = \mp k\phi^{(1)}_1 - \sigma_{\pm} k n^{(1)}_{\pm,1}, \tag{10}$$

$$-k^2\phi^{(1)}_1 = n^{(1)}_{-,1} - n^{(1)}_{+,1}. \tag{11}$$

This system of equations determines the dispersion relation

$$\frac{1}{(\sigma_+ k^2 - \omega^2)} + \frac{1}{(\sigma_- k^2 - \omega^2)} + 1 = 0, \tag{12}$$

of electrostatic wave in a pair-ion plasma. Solving this dispersion relation, we get two distinct modes of electrostatic wave in terms of frequency square (ω^2), which is defined as

$$\omega^2 = 1 + k^2 \pm \sqrt{1 + (1 - \sigma_+\sigma_-)k^4}. \tag{13}$$

When the wave number k is very small, these modes behave as

$$\omega^2 \cong k^2, \tag{14}$$

and

$$\omega^2 \cong 2 + k^2. \tag{15}$$

In dimensional form, we obtain the two modes as observed by experiment,[18] namely, low frequency ion acoustic wave (lower mode) $\omega^2 = C_s^2 k^2$ and high frequency ion plasma wave (upper mode) $\omega^2 = 2\omega_p^2 + C_s^2 k^2$. The graphical representation of Eq. (13) with plasma parameters $T_+ = 0.5$ eV and $T_- = 0.9$ eV is depicted in Fig. 1. The curves in this figure are in qualitative agreement with the modes observed in experiments.

The third mode in pair-ion plasmas, i.e., intermediate-frequency wave (IFW), which is observed in experiment,[18] cannot be obtained in theory in the present studies. IFW has a strange feature that its group velocity is negative and phase velocity is positive, i.e., the mode is like a backward mode. However, Vranjes *et al.*[27] have studied a backward mode in pair-ion plasmas with electron impurities. They have shown that the electron plasma mode may become a backward mode in the presence of a density gradient.

In the second order (n = 2), first harmonics (l = 1), we obtain the following relations in the matrix form:

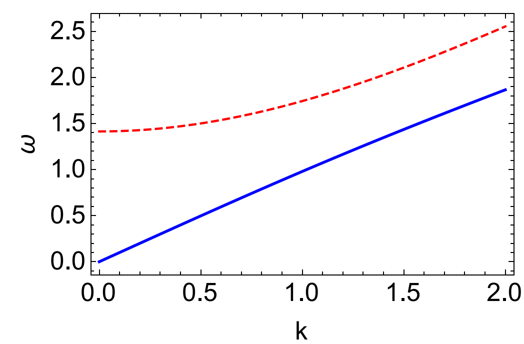

FIG. 1. Numerical solution of Eq. (13) for temperatures $T_+ = 0.5$ eV and $T_- = 0.9$ eV. In this figure, the blue line denotes the ion acoustic wave (lower mode) and the dotted red line denotes the ion plasma wave (upper mode).

$$\left[n^{(2)}_{\pm,1}, u^{(2)}_{\pm,1}\right]^T = \pm i(k\lambda - \omega) \times \left[\frac{2\omega k}{(\sigma_\pm k^2 - \omega^2)^2}, \frac{(\sigma_\pm k^2 + \omega^2)}{(\sigma_\pm k^2 - \omega^2)^2}\right]^T \frac{\partial \phi^{(1)}_1}{\partial \xi} \mp \left[\frac{k^2}{(\sigma_\pm k^2 - \omega^2)}, \frac{wk}{(\sigma_\pm k^2 - \omega^2)}\right]^T \phi^{(2)}_1, \tag{16}$$

where the superscript T represents the transpose of the matrix. We also deduce the following group velocity term by the compatibility condition:

$$\lambda = \frac{\partial\omega}{\partial k} = \frac{\omega}{k} - \frac{1}{\omega k\left[\frac{1}{(\sigma_+ k^2 - \omega^2)^2} + \frac{1}{(\sigma_- k^2 - \omega^2)^2}\right]}. \tag{17}$$

For next order (n = 2), we obtain the second-harmonic modes (l = 2) in terms of $\phi^{(1)2}_1$

$$\left[\phi^{(2)}_2,\ n^{(2)}_{+,2},\ u^{(2)}_{+,2},\ n^{(2)}_{-,2},\ u^{(2)}_{-,2}\right]^T = [A,\ B,\ C,\ D,\ E]^T \phi^{(1)2}_1. \tag{18}$$

The expressions for A, B, C, D, E are given in Appendix A [see Eqs. (A1)–(A5)]. The second order zeroth-harmonic modes (n = 2 and 3; l = 0) that appear due to the self-interaction of the modulated carrier wave are obtained by the following relations:

$$\left[\phi^{(2)}_0,\ n^{(2)}_{+,0},\ u^{(2)}_{+,0},\ n^{(2)}_{-,0},\ u^{(2)}_{-,0}\right]^T = [A_1,\ B_1,\ C_1,\ B_1,\ D_1]^T |\phi^{(1)}_1|^2. \tag{19}$$

The expressions for A_1, B_1, C_1, D_1 are given in Appendix A [see Eqs. (A6)–(A9)]. Finally, in third order first-harmonic modes (n = 3, l = 1), the coefficient of $\phi^{(3)}_1$ is zero by the dispersion relation, and the following nonlinear Schrödinger equation (NLSE) for $\phi^{(1)}_1 [= \psi]$ is obtained:

$$i\frac{\partial\psi}{\partial\tau} + P\frac{\partial^2\psi}{\partial\xi^2} + Q|\psi|^2\psi + i\Gamma_c\psi = 0, \tag{20}$$

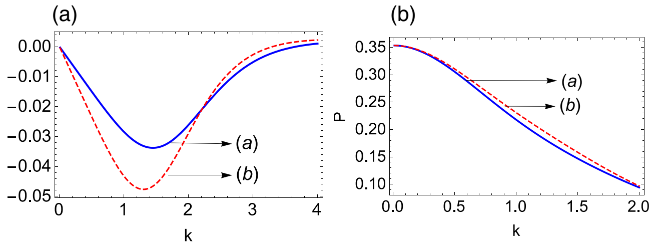

FIG. 2. Numerical solution of the variations of group dispersion coefficient P with respect to k derived from IAW (left figure) and IPW (right figure). The plasma parameters are (a) $T_+/T_- = 1.5$ and (b) $T_+/T_- = 0.6$.

with a dissipative term Γ_c. The coefficient P in the NLSE known as the group dispersion coefficient is related to the curvature of the dispersion relation $\omega(k)$ [Eq. (12)], and Q is related to the nonlinear frequency shift. For the high frequency ion plasmas wave, P and Q are always positive depending on the wave numbers k (Figs. 2 and 3). However, P is always negative and Q is both positive and negative for the low frequency ion acoustic wave depending on the wave numbers k (Figs. 2 and 3). The dissipative term

$$\Gamma_c = \frac{1}{2}\left(\frac{1}{(\sigma_+ k^2 - \omega^2)^2} + \frac{1}{(\sigma_- k^2 - \omega^2)^2}\right)^{-1} \times \left(\frac{\nu_+}{(\sigma_+ k^2 - \omega^2)^2} + \frac{\nu_-}{(\sigma_- k^2 - \omega^2)^2}\right), \tag{21}$$

is always positive for all wave numbers k (Fig. 4), which depends on the collision of ions with neutral particles. So, this dissipation term yields damping of the wave. We observe that from the expression of Γ_c, if the collision frequency $\nu_{\pm n}$ is zero, i.e., both ν_+ and ν_- are zero, then, the dissipative term Γ_c vanishes. Thus, for the collisionless system ($\Gamma_c = 0$), we can only get the NLSE without the dissipation term which generates a modulated wave with constant amplitude. On the other hand, for the collisional system ($\Gamma_c \neq 0$), we can get a damped NLSE, yielding a damped modulated wave whose amplitude decays with time.

IV. EFFECTS OF ION-NEUTRAL COLLISIONS ON MODULATION INSTABILITY

By assuming the fact that the neutral atoms collide with ions induces dissipation, the amplitude evolution equation (20) possesses the following plane-wave solution:

$$\psi = \psi_0(\tau) \exp\left[-i\int_0^{\tau} \Delta(\tau')d\tau'\right], \tag{22}$$

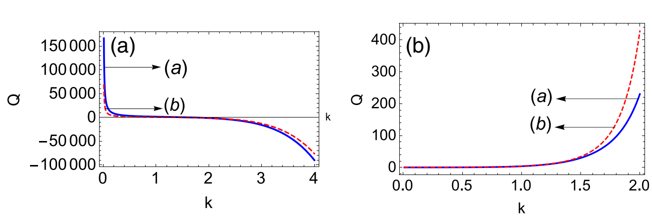

FIG. 3. Numerical solution of the variations of nonlinear coefficient Q with respect to k derived from IAW (left figure) and IPW (right figure). The plasma parameters are the same as Fig. 2.

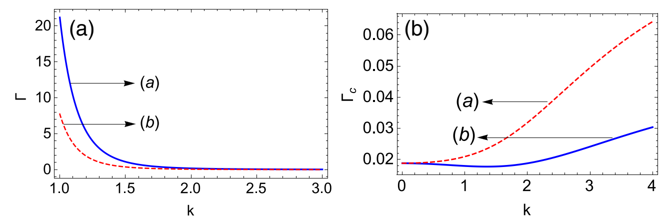

FIG. 4. Numerical solution of the variations of Γ_c with respect to k derived from IAW (left figure) and IPW (right figure). The plasma parameters are (a) $T_+/T_- = 1.5$, $\nu_+ = 0.01$, and $\nu_- = 0.02$ and (b) $T_+/T_- = 0.6$, $\nu_+ = 0.01$, and $\nu_- = 0.02$.

where $\psi_0(\tau)$ and $\Delta(\tau)$ are the amplitude of the pump carrier wave and the nonlinear frequency shift in the presence of dissipation, respectively. We have substituted this plane-wave solution in Eq. (20) and got the following two equations:

$$\frac{d\psi_0}{d\tau} + \Gamma_c\psi_0 = 0 \Rightarrow \psi_0(\tau) = \psi_{00}\exp[-\Gamma_c\tau], \tag{23}$$

and

$$\Delta(\tau) = -Q|\psi_0(\tau)|^2 = -Q|\psi_{00}|^2 \exp[-2\Gamma_c\tau], \tag{24}$$

where ψ_{00} is a real constant. Also, we have observed that $\psi_0(\tau) \to 0$ as $\tau \to \infty$ implies that ψ_0 is stable. For stability analysis, we consider the perturbation about this stable solution in the following standard procedure:

$$\psi = \left[\psi_0(\tau) + \tilde{\psi}(\xi,\tau)\right]\exp\left(-i\int_0^{\tau}\Delta(\tau')d\tau'\right), \tag{25}$$

where $\tilde{\psi}(|\tilde{\psi}| \ll \psi_0)$ is the perturbed amplitude of the modulated wave. Now, assuming a space-time dependence perturbation in the form $\tilde{\psi} \sim \exp(i\vartheta)$, where $\vartheta = \tilde{k}\xi - \int_0^{\tau}\tilde{\omega}(\acute{\tau})d\acute{\tau}$ is the modulated phase with the wave number $\tilde{k}(\ll k)$ and the modulation frequency $\tilde{\omega}(\ll \omega)$, from Eq. (20), we have obtained the following dispersion relation:

$$(\tilde{\omega} + i\Gamma_c)^2 = P^2\tilde{k}^4 - 2PQ|\psi_0|^2\tilde{k}^2. \tag{26}$$

From the dispersion relation [Eq. (26)], we have observed that the system is stable for $PQ < 0$. However, for $PQ > 0$, the system becomes unstable and the instability occurs known as modulational instability (or caviton instability in the case of one dimension).[34] For $PQ > 0$, we must have both P and Q are of the same sign. In this particular problem, we have both the cases $P < 0$, $Q < 0$ and $P > 0$, $Q > 0$ for some different k. Keeping the collision in the system, the instability could occur if

$$\tilde{k}^2 < \tilde{k}_{cr}^2 = \left(\frac{2Q}{P}\right)|\psi_0|^2, \tag{27}$$

which provides the following inequality:

$$\Gamma_c < \sqrt{P^2\tilde{k}^2\left(\frac{\tilde{k}_{cr}^2}{\tilde{k}^2} - 1\right)}. \tag{28}$$

This determines the maximum time τ_{max} to observe instability

$$\tau_{max} = \frac{1}{2\Gamma_c} \ln\left(\frac{2PQ\tilde{k}^2|\psi_{00}|^2}{\Gamma_c^2 + P^2\tilde{k}^4}\right), \tag{29}$$

which implies that the growth of instability will cease for $\tau \geq \tau_{max}$. In the case $PQ > 0$, we have obtained a dispersion relation

$$(\Gamma + \Gamma_c)^2 = 2PQ|\psi_0|^2\tilde{k}^2 - P^2\tilde{k}^4, \tag{30}$$

for the instability growth rate by putting $\tilde{\omega} = i\Gamma$ in Eq. (26). Therefore, the maximum value of $\tilde{k}^2$ is

$$\tilde{k}^2_{max} = \left(\frac{Q}{P}\right)|\psi_0|^2 = \left(\frac{Q}{P}\right)|\psi_{00}|^2 \exp\left(-2\Gamma_c\tau\right), \tag{31}$$

which yields the maximum growth rate

$$\Gamma_{max}(collisional) = \sqrt{2}|Q||\psi_0|^2 - \Gamma_c. \tag{32}$$

Thus, from the above relation, the instability occurs when $\sqrt{2}|Q||\psi_0|^2 > \Gamma_c$.

In the case of the collisionless system, we can put $\Gamma_c = 0$. So, in this case, it does not have any dissipation, and the dispersion relation of the modulated wave can be obtained by putting $\Gamma_c = 0$ in Eq. (26) which reads as

$$\tilde{\omega}^2 = P^2\tilde{k}^4 - 2PQ|\psi_{00}|^2\tilde{k}^2. \tag{33}$$

Also, the instability criteria for $PQ > 0$ can be obtained in the same way which is

$$\tilde{k}^2 < \tilde{k}^2_{cr} = \left(\frac{2Q}{P}\right)|\psi_{00}|^2, \tag{34}$$

and the maximum growth rate

$$\Gamma_{max}(collisionless) = \lim_{\Gamma_c \to 0} \Gamma_{max}(collisional) = \sqrt{2}|Q||\psi_{00}|^2. \tag{35}$$

Comparing both the cases of collisional and collisionless systems, we obtain

$$\Gamma_{max}(collisionless) > \Gamma_{max}(collisional),$$

as $\Gamma_c > 0$.

V. SOLITON SOLUTIONS

In the above damped NLSE [Eq. (20)], for the ion acoustic mode, the group dispersion coefficient P [Eq. (A10)] is negative, and for the ion plasma mode, P is positive for small wave number k. However, for the ion acoustic mode, the nonlinear coefficient Q [Eq. (A11)] is both positive and negative depending on the wave number k, and for the ion plasma mode, Q is always positive. Now, to get the soliton solutions of the damped NLSE [Eq. (20)], we have normalized the equation in the following form:

$$i\frac{\partial\psi}{\partial\bar{\tau}} + \frac{1}{2}\kappa_d\frac{\partial^2\psi}{\partial\bar{\xi}^2} + \kappa_n|\psi|^2\psi + i\varepsilon(\psi) = 0, \tag{36}$$

where $\bar{\tau} = |Q|\tau, \bar{\xi} = \xi\sqrt{|Q|/2|P|}, \varepsilon(\psi) = \Gamma_c\psi/|Q|$, and $\kappa_d = \kappa_n = \pm 1$. The solutions of the normalized NLSE [Eq. (36)] determine nonlinear excitations, in the form of bright and dark solitons. This equation yields bright or envelope solitons for $\kappa_d = -1, \kappa_n = -1$, and $\kappa_d = +1, \kappa_n = +1$, whereas it gives dark solitons for $\kappa_d = -1, \kappa_n = +1$. We have solved Eq. (36) numerically for $\kappa_d = \pm 1, \kappa_n = \pm 1$ and also analytically. Analytical solutions in each cases are shown in following Subsections.

A. Bright soliton: Collisionless pair-ion plasmas

In the case of collisionless pair-ion plasmas, collisional frequency is zero, i.e., $\nu_\pm = 0$, and so, $\Gamma_c = 0$. Therefore, we can put $\varepsilon(\psi) = 0$ in Eq. (36). Now, we have the usual NLSE which is solved for the two different sets of values of κ_d and κ_n, which are $\kappa_d = \kappa_n = -1$ and $\kappa_d = \kappa_n = +1$. Solutions of this NLSE can be obtained using the inverse scattering transform. Let us consider that a solution is of the form $\psi(y,t) = \sqrt{\rho(y)}\exp[i\varphi(y,t)]$, where $y = \bar{\xi} - V\bar{\tau}$ is a travelling wave coordinate and $t = \bar{\tau}$. Therefore, the amplitude of the wave envelope, $|\psi| = \sqrt{\rho}$, is a travelling wave, moving with the group velocity λ plus the velocity V. After separating the real and imaginary parts, we solve the ordinary differential equation for φ and ρ (with the boundary condition $\rho \to 0$ as $\xi \to \pm\infty$). Finally, we obtain the following single bright solitons which are in terms of actual parameters:

$$\psi(\xi,\tau) = a\,\mathrm{sech}\left[a\sqrt{\frac{|Q|}{2|P|}}\left(\xi - \sqrt{2|PQ|}V\tau\right)\right] \times \exp\left[is_1\sqrt{\frac{|Q|}{2|P|}}\left(V\xi + \sqrt{\frac{|PQ|}{2}}(a^2 - V^2)\tau\right)\right], \tag{37}$$

where V is the velocity and "a" is the amplitude of the soliton. In the above solution, $s_1 = +1$ for the set $\kappa_d = \kappa_n = -1$ and $s_1 = -1$ for the set $\kappa_d = \kappa_n = +1$. This soliton shows that after they experience the collisions, they emerge with the same shape and velocity, also having an exponential factor, making the oscillation between maxima and minima. Numerically, a single bright soliton is depicted in Fig. 5 for different plasma parameters.

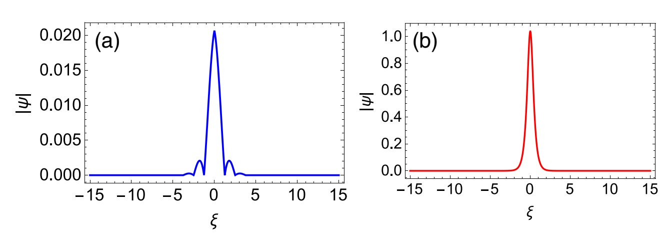

FIG. 5. Numerical solution of the bright (envelope) soliton of Eq. (20) derived from IAW (left figure) for $k = 3.0$ and IPW (right figure) for $k = 1.0$. Both figures are derived for the plasma parameter $T_+/T_- = 0.6$.

B. Bright soliton: Collisional pair-ion plasmas

In the case of collisional pair-ion plasmas, the collisional frequency, $\nu_{\pm} \neq 0$, and therefore, $\Gamma_c \neq 0$. With this damping term ($\Gamma_c \neq 0$), Eq. (36) is not a completely integrable Hamiltonian system, and therefore, the system is not exactly solvable. However, we can obtain an approximate analytical solution of the damped NLSE [Eq. (36)] by using soliton perturbation analysis.[35,36] Therefore, we have assumed that the amplitude of the soliton is time dependent, and the general solution of this perturbed soliton is as follows:

$$\psi(\bar{\xi},\bar{\tau}) = a(\bar{\tau})\mathrm{sech}\left[a(\bar{\tau})\left(\bar{\xi} - b(\bar{\tau})\right)\right] \times \exp\left[is_1\bar{\xi}\bar{V}(\bar{\tau}) + is_1\sigma(\bar{\tau})\right], \tag{38}$$

where a, b, σ, and $\bar{V}$ are the time dependent soliton parameters. Finally, applying the conservation laws for the NLSE (conserved integral relations), we obtain the following bright soliton (envelope soliton) in the presence of ion-neutral collision, which in terms of actual variable reads as

$$\psi(\xi,\tau) = a_0\exp(-2\Gamma_c\tau)\mathrm{sech}\left[a_0\exp(-2\Gamma_c\tau)\sqrt{\frac{|Q|}{2|P|}}\left(\xi - \sqrt{2|PQ|}V_0\tau\right)\right] \times \exp\left[is_1\sqrt{\frac{|Q|}{2|P|}}\left[V_0\xi - \sqrt{\frac{|PQ|}{2}}\left(a_0^2\left(\frac{\exp(-4\Gamma_c\tau)-1}{4\Gamma_c}\right) - V_0^2\tau\right)\right]\right], \tag{39}$$

where a_0 and V_0 are the initial values of a and V, respectively. In the limit $\Gamma_c \to 0$, we recover the previous result [Eq. (37)] (with $a_0 = a$ and $V_0 = V$). It is clear that as time elapses, the amplitude of the bright (envelope) soliton decreases exponentially with a decay rate $\sim 2\Gamma_c$. The numerical solution in Fig. 6 also shows similar nature.

C. Dark soliton: Collisionless pair-ion plasmas

In this case, we have solved the NLSE [Eq. (36)] for $\kappa_d = -1, \kappa_n = +1$. Proceeding as before, we have obtained the dark soliton using inverse scattering transformation subject to the boundary condition $\rho \to a$ (a constant). Finally, we obtain a solution which is in actual parameter looks like[35,36]

$$\psi(\xi,\tau) = aK\sqrt{\tanh^2(\zeta) + \frac{(1-K^2)}{K^2}}\exp\left[i\sqrt{\frac{|Q|}{2|P|}}\left(\left(V + a\sqrt{1-K^2}\right)\xi - \sqrt{\frac{|PQ|}{2}}\left(a^2(3-K^2) + 2aV\sqrt{1-K^2} + V^2\right)\tau\right) + \eta\right], \tag{40}$$

where $\zeta = \left[aK\sqrt{|Q|/2|P|}\left(\xi - \sqrt{2|PQ|}V\tau\right)\right]$ and $\eta = \tan^{-1}\left[\frac{K}{\sqrt{1-K^2}}\tanh(\zeta)\right]$ and "a" is the amplitude of the dark soliton, V is the velocity of dark soliton, and K($0 < K \leq 1$) is an arbitrary parameter. Numerically, a single dark soliton is depicted in Fig. 7. Generally, dark solitons are also called a gray soliton when $|K| < 1$ and a black soliton when $|K| = 1$. So, in the case of $|K| = 1$, from the above equations, we get black solitons as

$$\psi(\xi,\tau) = a\tanh\left[a\sqrt{\frac{|Q|}{2|P|}}\left(\xi - \sqrt{2|PQ|}V\tau\right)\right] \times \exp\left[i\sqrt{\frac{|Q|}{2|P|}}\left(V\xi - \sqrt{\frac{|PQ|}{2}}(2a^2 + V^2)\tau\right)\right]. \tag{41}$$

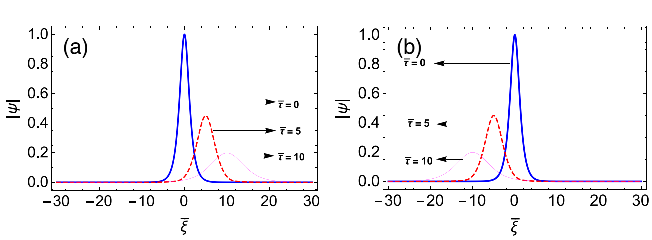

FIG. 6. Numerical solution of the bright (envelope) soliton of Eq. (36) derived from IAW (left figure) and IPW (right figure) in the presence of dissipation ($\Gamma_c = 0.1$) due to the collision.

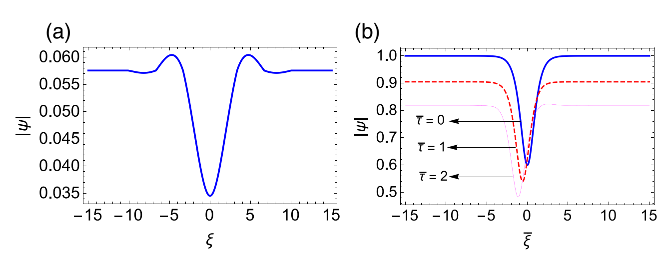

FIG. 7. Numerical solution of the dark (envelope) soliton of Eq. (20) derived from IAW (left figure) for $k = 1.0$ and $T_+/T_- = 0.6$. The numerical solution of the dark (envelope) soliton of Eq. (36) is derived from IAW (right figure) in the presence of dissipation ($\Gamma_c = 0.1$) due to the collision.

D. Dark soliton: Collisional pair-ion plasmas

With this damping term ($\Gamma_c \neq 0$), Eq. (36) is not a completely integrable Hamiltonian system, and so, the system is not exactly solvable. Therefore, as earlier, we have assumed that the amplitude of the soliton is time dependent, and general solutions of dark (black) solitons are as follows:[37,38]

$$\psi(\bar{\xi},\bar{\tau}) = a(\bar{\tau})\tanh\left[a(\bar{\tau})\left(\bar{\xi} - b(\bar{\tau})\right)\right] \exp\left[i\bar{\xi}\bar{V}(\bar{\tau}) - i\sigma(\bar{\tau})\right], \quad (42)$$

where a, b, σ, and $\bar{V}$ are the time dependent soliton parameters. Now, applying the conservation laws for the NLSE, we have obtained

$$a(\bar{\tau}) = a_0 \exp\left(-\Gamma_c\bar{\tau}\right); \quad V(\bar{\tau}) = V_0 \exp\left(-\Gamma_c\bar{\tau}\right), \quad (43)$$

where a_0 and V_0 are the initial values of a and V, respectively. The dark soliton amplitude also decays exponentially with time having a decay rate $\sim\Gamma_c$ due to the ion-neutral collision. The numerical solution in Fig. 7 also shows similar nature. In this case, the decay rate is half of that of the bright soliton. In the limit $\Gamma_c \to 0$, we recover the usual single dark soliton [Eq. (41)].

VI. CONCLUSIONS

In the preceding sections, we have demonstrated the nonlinear dynamics of the propagating IAWs and IPWs in the absence of the magnetic field in collisional pair-ion plasmas, by applying a two-fluid plasma model. The electrostatic wave packets are governed by a damped NLSE. The damping originates due to the ion-neutral collision. To observe the collisional effect on electrostatic wave modulation, we have assumed that $\frac{\nu_{\pm n}}{\omega_p} \sim \nu_{\pm}\epsilon^2$ so that the collisional frequency is much smaller than the plasma frequency.

In our present study, we have obtained two distinct electrostatic modes, namely, a low frequency ion acoustic mode (lower mode) and a high frequency ion plasma mode (upper mode), where the temperature of the two ions is slightly different. These modes are observed by previous experiments,[20–23] and here, also we get exactly the same modes. Adopting the standard reductive perturbation technique, the basic set of equations reduces to the dissipative (here damped) nonlinear Schrödinger equation (NLSE) for the slowly varying electric potential. The ion-neutral collision is responsible for the dissipation on the governed NLSE. In the absence of collision, the present analysis reveals that the ion acoustic mode is either stable or unstable depending upon the wave number k. In the region $PQ < 0$, the ion acoustic mode is stable and propagates in the form of a dark (envelope) soliton. In the region $PQ > 0$, the ion acoustic mode is unstable and propagates in the form of a bright (envelope) soliton. However, the ion plasma mode is always unstable and propagates in the form of a bright envelope soliton. In the presence of collision, the amplitudes of bright and dark envelope solitons decrease exponentially with respect to time with decay rates $\sim 2\Gamma_c$ and $\sim\Gamma_c$, respectively. Finally, the results of our investigation could be useful to understand the modulated electrostatic waves in fullerene pair-ion plasmas.

In connection with the equal mass pair-ion plasma experiment, we must mention that we have not encountered any experimental observations of the nonlinear structures in pure pair-ion plasmas. However, many authors[39–45] have studied nonlinear waves (including wave modulations) in multi-component plasmas consisting of electrons and positive and negative ions. The experimental observations reveal that the amplitude of the density fluctuation $n_1/n_0 \sim 0.1$ is sufficient to observe nonlinear wave phenomena in laboratory plasmas. Moreover, the experimental results are well explained by the small amplitude (weakly nonlinear) theoretical analysis. Recently, pure pair-ion plasmas (without electrons) consisting of fullerene ions are observed in experiment.[20–23] The masses of both the ions (positive and negative) are equal because they are generated by the same source (fullerene ion source), but their temperatures are slightly different due to the different charging processes of both the positive and negative fullerene ions.[20–23] Thus, we expect that in future, the nonlinear wave phenomena could be observed in such a plasma system, provided that the amplitude of the fluctuations are $\gtrsim 0.1$. Also, the investigation of collective phenomena in pair-ion plasmas is extremely important from a diagnostic point of view, and thus, the findings of the present investigation can be used in diagnosing the pair-ion plasmas.

APPENDIX A: EXPRESSIONS OF DIFFERENT COEFFICIENTS

$$A = \frac{k^2}{6}\left[\frac{(\sigma_- k^2 + 3\omega^2)}{(\sigma_- k^2 - \omega^2)^3} - \frac{(\sigma_+ k^2 + 3\omega^2)}{(\sigma_+ k^2 - \omega^2)^3}\right], \quad (A1)$$

$$B = -\frac{k^2}{(\sigma_+ k^2 - \omega^2)}\left[A + \frac{1}{2}\frac{(\sigma_+ k^2 + 3\omega^2)k^2}{(\sigma_+ k^2 - \omega^2)^2}\right], \quad (A2)$$

$$C = \left[\frac{\omega}{k}B - \frac{\omega k^3}{(\sigma_+ k^2 - \omega^2)^2}\right], \quad (A3)$$

$$D = \frac{k^2}{(\sigma_- k^2 - \omega^2)}\left[A - \frac{1}{2}\frac{(\sigma_- k^2 + 3\omega^2)k^2}{(\sigma_- k^2 - \omega^2)^2}\right], \quad (A4)$$

$$E = \left[\frac{\omega}{k}D - \frac{\omega k^3}{(\sigma_- k^2 - \omega^2)^2}\right], \quad (A5)$$

$$A_1 = \frac{1}{2(1-\lambda^2)}\left[(\sigma_+ - \lambda^2)\frac{2\lambda\omega k^3 + \omega^2 k^2 + \sigma_- k^4}{(\sigma_- k^2 - \omega^2)^2}, - (\sigma_- - \lambda^2)\frac{2\lambda\omega k^3 + \omega^2 k^2 + \sigma_+ k^4}{(\sigma_+ k^2 - \omega^2)^2}\right], \quad (A6)$$

$$B_1 = \frac{1}{(\lambda^2 - \sigma_+)}\left[A_1 + \frac{2\lambda\omega k^3 + \omega^2 k^2 + \sigma_+ k^4}{(\sigma_+ k^2 - \omega^2)^2}\right], \quad (A7)$$

$$C_1 = \left[\lambda B_1 - \frac{2\omega}{k}\frac{k^4}{(\sigma_+ k^2 - \omega^2)^2}\right], \quad (A8)$$

$$D_1 = \left[\lambda B_1 - \frac{2\omega}{k}\frac{k^4}{(\sigma_- k^2 - \omega^2)^2}\right]. \tag{A9}$$

The group dispersion coefficient P is given by

$$P = -\frac{1}{2}\left[\frac{\lambda}{\omega k}(k\lambda - \omega) + \frac{4\omega}{k}(k\lambda - \omega)^2 \times \left[\frac{(\sigma_- k - \omega\lambda)}{(\sigma_- k^2 - \omega^2)^3} + \frac{(\sigma_+ k - \omega\lambda)}{(\sigma_+ k^2 - \omega^2)^3}\right]\right] = \frac{1}{2}\frac{\partial^2 \omega(k)}{\partial k^2}. \tag{A10}$$

The coefficient of the nonlinear term Q is given by

$$Q = \frac{(k\lambda - \omega)}{2}\left[\frac{2\omega k(C + C_1)}{(\sigma_+ k^2 - \omega^2)^2} + \frac{2\omega k(E + D_1)}{(\sigma_- k^2 - \omega^2)^2} + \frac{(\sigma_+ k^2 + \omega^2)(B + B_1)}{(\sigma_+ k^2 - \omega^2)^2} + \frac{(\sigma_- k^2 + \omega^2)(D + B_1)}{(\sigma_- k^2 - \omega^2)^2}\right]. \tag{A11}$$

APPENDIX B: OUTLINES OF THE CALCULATIONS

Substitution of Eqs. (6)–(8) in Eqs. (3)–(5) yields the following n-th order reduced set of equations:

$$-il\omega n_{\pm,l}^{(n)} - \lambda\frac{\partial n_{\pm,l}^{(n-1)}}{\partial\xi} + \frac{\partial n_{\pm,l}^{(n-2)}}{\partial\tau} + ilku_{\pm,l}^{(n)} + \frac{\partial u_{\pm,l}^{(n-1)}}{\partial\xi} + \sum_{n'=1}^{\infty}\sum_{l'=-\infty}^{\infty}\left[ilku_{\pm,l'}^{(n')}n_{\pm,l-l'}^{(n-n')} + \frac{\partial}{\partial\xi}\left(u_{\pm,l'}^{(n')}n_{\pm,l-l'}^{(n-n'-1)}\right)\right] = 0, \tag{B1}$$

$$-il\omega u_{\pm,l}^{(n)} \pm ilk\phi_l^{(n)} + \sigma_\pm ilkn_{\pm,l}^{(n)} - \lambda\frac{\partial u_{\pm,l}^{(n-1)}}{\partial\xi} \pm \frac{\partial\phi_l^{(n-1)}}{\partial\xi} + \sigma_\pm\frac{\partial n_{\pm,l}^{(n-1)}}{\partial\xi} + \nu_\pm u_{\pm,l}^{(n-2)} + \frac{\partial u_{\pm,l}^{(n-2)}}{\partial\tau} + \frac{1}{2}\sum_{n'=1}^{\infty}\sum_{l'=-\infty}^{\infty}\left[ilku_{\pm,l'}^{(n')}u_{\pm,l-l'}^{(n-n')} + \frac{\partial}{\partial\xi}\left(u_{\pm,l'}^{(n')}u_{\pm,l-l'}^{(n-n'-1)}\right) + \sigma_\pm\left[ilkn_{\pm,l'}^{(n')}n_{\pm,l-l'}^{(n-n')} + \frac{\partial}{\partial\xi}\left(n_{\pm,l'}^{(n')}n_{\pm,l-l'}^{(n-n'-1)}\right)\right]\right] = 0, \tag{B2}$$

$$-l^2k^2\phi_l^{(n)} + 2ilk\frac{\partial\phi_l^{(n-1)}}{\partial\xi} + \frac{\partial^2\phi_l^{(n-2)}}{\partial\xi^2} = n_{-,l}^{(n)} - n_{+,l}^{(n)}. \tag{B3}$$

[1]D. H. E. Dubin, Phys. Rev. Lett. **92**, 195002 (2004).
[2]N. Iwamoto, Phys. Rev. E **47**, 604 (1993).
[3]U. A. Mofiz, Phys. Rev. A **40**, 2203 (1989).
[4]I. Kourakis, A. Esfandyari-Kalejahi, M. Mehdipoor, and P. K. Shukla, Phys. Plasmas **13**, 052117 (2006).
[5]R. Sabry, W. M. Moslem, P. K. Shukla, and H. Saleem, Phys. Rev. E **79**, 056402 (2009).
[6]J. Zhao, J. I. Sakai, and K. I. Nishikawa, Phys. Plasmas **3**, 844 (1996).
[7]R. Sabry, Phys. Plasmas **15**, 092101 (2008).
[8]C. M. Surko, M. Leventhal, and A. Passner, Phys. Rev. Lett. **62**, 901 (1989).
[9]R. G. Greaves, M. D. Tinkle, and C. M. Surko, Phys. Plasmas **1**, 1439 (1994).
[10]H. Boehmer, M. Adams, and N. Rynn, Phys. Plasmas **2**, 4369 (1995).
[11]M. Amoretti, C. Amsler, G. Bonomi, A. Bouchta, P. D. Bowe, C. Carraro, C. L. Cesar, M. Charlton, M. Doser, V. Filippini *et al.*, Phys. Rev. Lett. **91**, 055001 (2003).
[12]F. C. Michel, *Theory of Neutron Star Magnetospheres* (Chicago University Press, Chicago, 1991).
[13]P. Goldreich and W. H. Julian, Astrophys. J. **157**, 869 (1969).
[14]M. J. Rees, in *The Early Universe*, edited by G. W. Gibbons, S. W. Hawking, and S. Siklas (Cambridge University Press, Cambridge, 1983).
[15]H. R. Miller and P. J. Witta, *Active Galactic Nuclei* (Springer-Verlag, Berlin 1987), p. 202.
[16]E. P. Liang, S. C. Wilks, and M. Tabak, Phys. Rev. Lett. **81**, 4887 (1998).
[17]W. M. Moslem and P. K. Shukla, Phys. Plasmas **13**, 122104 (2006).
[18]W. Oohara, D. Date, and R. Hatakeyama, Phys. Rev. Lett. **95**, 175003 (2005).
[19]P. K. Shukla and L. Stenflo, Phys. Plasmas **12**, 044503 (2005).
[20]W. Oohara and R. Hatakeyama, Phys. Rev. Lett. **91**, 205005 (2003).
[21]W. Oohara, Y. Kuwabara, and R. Hatakeyama, Phys. Rev. E **75**, 056403 (2007).
[22]W. Oohara and R. Hatakeyama, Phys. Plasmas **14**, 055704 (2007).
[23]R. Hatakeyama and W. Oohara, Phys. Scr. **T116**, 101 (2005).
[24]J. Vranjes and S. Poedts, Plasma Sources Sci. Technol. **14**, 485 (2005).
[25]G. P. Zank and R. G. Greaves, Phys. Rev. E **51**, 6079 (1995).
[26]H. J. Ren, J. Cao, and Z. Wu, Phys. Plasmas **15**, 102108 (2008).
[27]J. Vranjes, D. Petrovic, B. P. Pandey, and S. Poedts, Phys. Plasmas **15**, 072104 (2008).
[28]W. Oohara, H. Iwata, D. Date, and R. Hatakeyama, Thin Solid Films **475**, 49 (2005); W. Oohara and R. Hatakeyama, *ibid.* **435**, 280 (2003).
[29]W. Oohara, H. Iwata, and R. Hatakeyama, Surf. Coat. **201**, 5446 (2007).
[30]E. E. B. Campbell, V. Schyja, R. Ehlich, and I. V. Hertel, Phys. Rev. Lett. **70**, 263 (1993).
[31]M. Salahuddin, H. Saleem, and M. Saddiq, Phys. Rev. E **66**, 036407 (2002).
[32]J. D. Huba, *NRL Plasma Formulary* (Naval Research Laboratory, Washington, DC, 2000).
[33]T. Taniuti and N. Yajima, J. Math. Phys. **10**, 1369 (1969); N. Asano, T. Taniuti, and N. Yajima, J. Math. Phys. **10**, 2020 (1969).
[34]P. M. Bellan, *Fundamentals of Plasma Physics* (Cambridge University Press, Cambridge, 2006).
[35]A. Hasegawa and Y. Kodama, *Solitons in Optical Communications* (Clarendon, Oxford, 1995).
[36]Y. S. Kivshar and G. P. Agarwal, *Optical Solitons: From Fibres to Photonic Crystals* (Academic, San Diego, 2003).
[37]M. Lisak, D. Anderson, and B. A. Malomed, Opt. Lett. **16**, 1936 (1991).
[38]Y. S. Kivshar and X. Yang, Phys. Rev. E **49**, 1657 (1994).
[39]Y. Nakamura, J. Plasma Phys. **38**, 461–471 (1987).
[40]H. Ikezi, Phys. Fluids **16**, 1668 (1973).
[41]M. Q. Tran, Phys. Scr. **20**, 317–327 (1979).
[42]H. Bailung and Y. Nakamura, J. Plasma Phys. **50**, 231 (1993).
[43]H. Bailung, S. K. Sharma, and Y. Nakamura, Phys. Rev. Lett. **107**, 0255005 (2011).
[44]S. K. Sharma and H. Bailung, J. Geophys. Res. **118**, 919, https://doi.org/10.1002/jgra.50111 (2013).
[45]P. Pathak, S. K. Sharma, Y. Nakamura, and H. Bailung, Phys. Plasmas **23**, 022107 (2016).